ELSEVIER

PII: S0032-3861(97)10075-1

Polymer Vol. 39 No. 21, pp. 5093–5104, 1998
0032-3861/98/$ – see front matter

Melting of polymer crystals observed by temperature modulated d.s.c. and its kinetic modelling

Akihiko Toda[a,*], Chiyoko Tomita[a], Masamichi Hikosaka[b] and Yasuo Saruyama[a]
[a]*Faculty of Integrated Arts and Sciences, Hiroshima University, 1-7-1 Kagamiyama, Higashi-Hiroshima, 739, Japan*
[b]*Faculty of Textile Science, Kyoto Institute of Technology, Matsugasaki, Sakyo-ku, Kyoto, 606, Japan*
(Received 28 July 1997; revised 2 September 1997; accepted 10 September 1997)

Irreversible melting of poly(ethylene terephthalate) crystals on heating has been examined by temperature modulated differential scanning calorimetry (t.m.d.s.c.). The apparent heat capacity of complex quantity obtained by t.m.d.s.c. showed a strong dependence on frequency and heating rate during the melting process. In order to explain this behavior, a kinetic modelling of melting has been presented. The modelling considers the melting of an assembly of fractions having a continuous distribution of non-equilibrium melting points. Three cases of the superheating dependence of melting rate coefficient have been examined: constant rate coefficient, linear dependence and exponential dependence. The modelling predicts frequency response functions similar to Debye's type with a characteristic time dependent on heating rate. The response function successfully explains the dependence on frequency and heating rate of the apparent heat capacity obtained experimentally. The characteristic time of melting of crystallites has been evaluated as a fitting parameter of the response function, and the superheating dependence of melting rate coefficient has been distinguished by the heating rate dependence of the characteristic time. Taking account of the relatively insensitive nature of crystallization to temperature modulation, it is further suggested that the 'reversing' heat flow is related to the pure endothermic heat flow of melting and the 'non-reversing' heat flow corresponds to the exothermic heat flow of re-crystallization and re-organization when extrapolated to $\omega \rightarrow 0$. The behavior of the apparent heat capacity will be an important characteristic feature of the melting kinetics, and hence the modelling will develop a new applicability of t.m.d.s.c. to the melting of polymer crystals.

(Keywords: temperature modulated d.s.c.; kinetics of melting; polymer crystals)

INTRODUCTION

Temperature modulated differential scanning calorimetry (t.m.d.s.c.)[1–6] is a new technique applying a sinusoidal temperature modulation on a linear heating/cooling of conventional d.s.c. and analyzes the relationship between the modulation components of sample temperature, T_s, and of heat flow, $\dot{Q}$, expressed as,

$$T_s = \bar{T}_s + \tilde{T}_s e^{i(\omega t + \epsilon)} \tag{1}$$

$$\dot{Q} = \bar{\dot{Q}} + \tilde{\dot{Q}} e^{i(\omega t + \delta)} \tag{2}$$

From the amplitude and phase of the modulation components, we can define an apparent heat capacity of complex quantity, $\widetilde{\Delta C} e^{-i\alpha}$, whose magnitude and phase are defined as follows[7–9],

$$\widetilde{\Delta C} = \frac{\tilde{\dot{Q}}}{\omega \tilde{T}_s} \tag{3}$$

$$\alpha = (\epsilon - \delta) - (\epsilon - \delta)_0 \tag{4}$$

where $(\epsilon - \delta)_0$ represents the baseline of the phase lag.

Figure 1 shows a typical example of the change in the magnitude and phase obtained by a heating and cooling run of amorphous poly(ethylene terephthalate) (PET). Corresponding to the change in the total heat flow which is equivalent to the heat flow of conventional d.s.c., the changes are clearly seen for the glass transition, cold crystallization and melting in the heating run and the ordinary crystallization in the subsequent cooling run. The changes both in the magnitude and phase become quite large for the melting process, while the apparent heat capacity is relatively insensitive to the crystallization process.

For an irreversible kinetics of exo- or endothermic process such as crystallization or melting under supercooled or superheated condition, we have recently proposed the following expression for the apparent heat capacity given by the contribution of true heat capacity and of the kinetic response[7–9],

$$\widetilde{\Delta C} e^{-i\alpha} = mc_p + i\frac{1}{\omega} F_T' \tag{5}$$

Here, mc_p is given by the specific heat, c_p, multiplied by the sample weight, m, and F'_T represents the temperature derivative of the irreversible exo- or endothermic heat flow. As well as the magnitude of the apparent heat capacity, ΔC, we consider the change in the phase angle, α, which has been overlooked in the conventional analysis of t.m.d.s.c.

In a series of our experimental works[7–10], we have applied the model to the crystallization process of polymers.

* To whom correspondence should be addressed

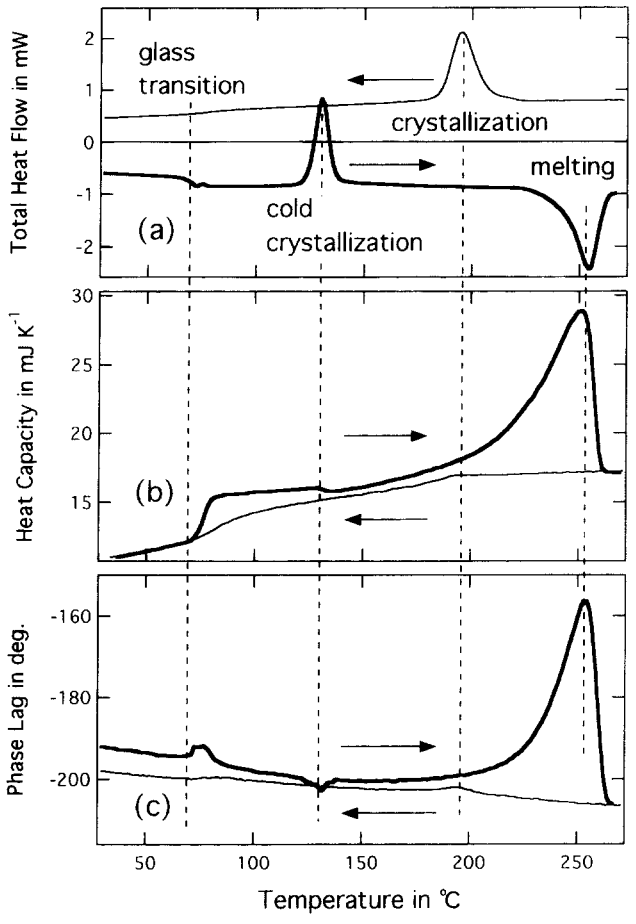

Figure 1 T.m.d.s.c. of heating (thick line) and cooling (thin line) runs of amorphous PET of 9.44 mg at 3.0 K min^{-1}: (a) total heat flow $\bar{Q}$, (b) magnitude of the apparent heat capacity $\widetilde{\Delta C}$ and (c) the phase lag ($\epsilon - \delta$). The modulation period was 28 s

We have examined the crystallization of polyethylene[7,10] and PET [8,9] under quasi-isothermal (constant $\bar{T}_s$) and non-isothermal ($\bar{T}_s = \beta t$) conditions. The frequency dependence of $\widetilde{\Delta C} e^{-i\alpha}$ was well approximated by the following expression,

$$\widetilde{\Delta C} e^{-i\alpha} = A + i\frac{B}{\omega} \tag{6}$$

where A and B are real quantities independent of ω. Utilizing the simple frequency dependence, the model proved its usefulness especially in the determination of the temperature dependence of crystal growth rate[7-10].

In the present paper, we examine the irreversible melting of polymer crystals on a heating run, $\bar{T}_s = \beta t$. Melting process is also of interest in the applicability of t.m.d.s.c., because the apparent heat capacity is quite sensitive to the melting process, as typically seen in *Figure 1* for PET and reported by Saruyama[11] for polyethylene. Hence, the information is expected to be valuable for further understanding of the melting process. However, the melting of polymer crystals is far more complicated than crystallization because of the fast kinetics, co-existence of re-crystallization and re-organization, and the wide distribution of the non-equilibrium melting points[12]. It is also known that, in the melting peak, the 'reversing' heat flow calculated from the magnitude of the apparent heat capacity, $-\beta\widetilde{\Delta C}(\omega)$, becomes larger than the total heat flow, $\bar{Q}$, as shown in *Figure 2*. Here, the total heat flow comprises the contribution of the true heat capacity, $-\beta mc_p$, and

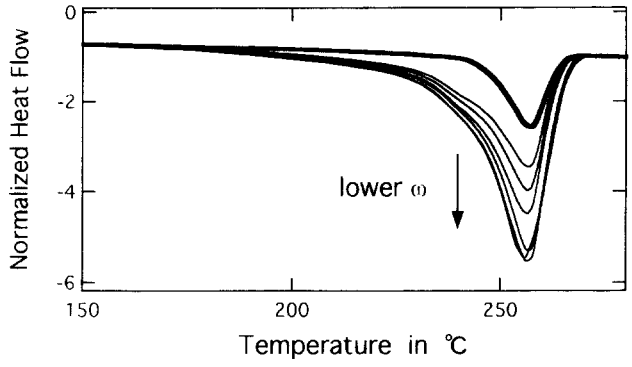

Figure 2 Plots of the 'reversing' heat flow $-\beta\widetilde{\Delta C}(\omega)$ for different modulation periods (thin lines, 36, 44, 56, 68, 84 and 100 s) along with the total heat flow $\bar{Q}$ (thick line) during the melting process of PET crystals. The heating rate was 3.0 K min^{-1}. The heat flow was normalized by the total heat flow of molten PET at 280°C. The sample weight was 2.47 mg

the underlying heat flow of transformation, $\bar{F}$: $\bar{Q} = -\beta mc_p + \bar{F}$. Therefore, if the 'reversing' heat flow is only of the contribution of the true heat capacity, mc_p, the relationship between the 'reversing' heat flow and the total heat flow means that the melting process is exothermic, namely $\bar{F} > 0$, which cannot be the case. The anomalous behavior of the 'reversing' heat flow must be due to the contribution of melting kinetics in the apparent heat capacity, which will be the main subject of the present paper.

In the following, we firstly examine the melting behavior of PET crystals, especially frequency and heating rate dependence of the apparent heat capacity during the melting process. Secondly, we discuss possible modelling of the melting kinetics and present a new analysis method of the melting process by t.m.d.s.c.

EXPERIMENTAL RESULTS

Experimental

The d.s.c. 2920 Module controlled with Thermal Analyst 2200 (TA Instruments) and equipped with a TA RMX Utility was used for all measurements. Nitrogen gas with a flow rate of 40 ml min^{-1} was purged through the cell. The phase, ϵ and δ, were calculated from the raw data of sample temperature and of heat flow. A modulation period of 24–100 s was examined with the modulation amplitude adjusted for the condition of heating only,

$$\frac{d\bar{T}_s}{dt} > 0 \left(\bar{T}_s < \frac{\beta}{\omega}\right).$$

In the figures, the data points are plotted at the interval of the applied modulation period.

The d.s.c. run of the present experiment consists of cyclic heating and cooling runs of a sample with different modulation periods at each heating rate. The cooling runs were at the rate of 10 K min^{-1} from the melt kept at 285°C, and the heating runs were from 100°C at the rate in the range of 0.7–4.5 K min^{-1}. In the data analysis of t.m.d.s.c., the apparent heat capacity was calibrated for different modulation periods, and the change in the calibration constants with temperature was also taken into account. The apparent heat capacity was then normalized by the value of molten PET at 280°C. The baseline of the phase lag, $(\epsilon - \delta)_0$, was determined by a straight line between the phase lags at 150°C and at the end of melting (~280°C). The choice of the baseline will not be crucial because the melting peaks in

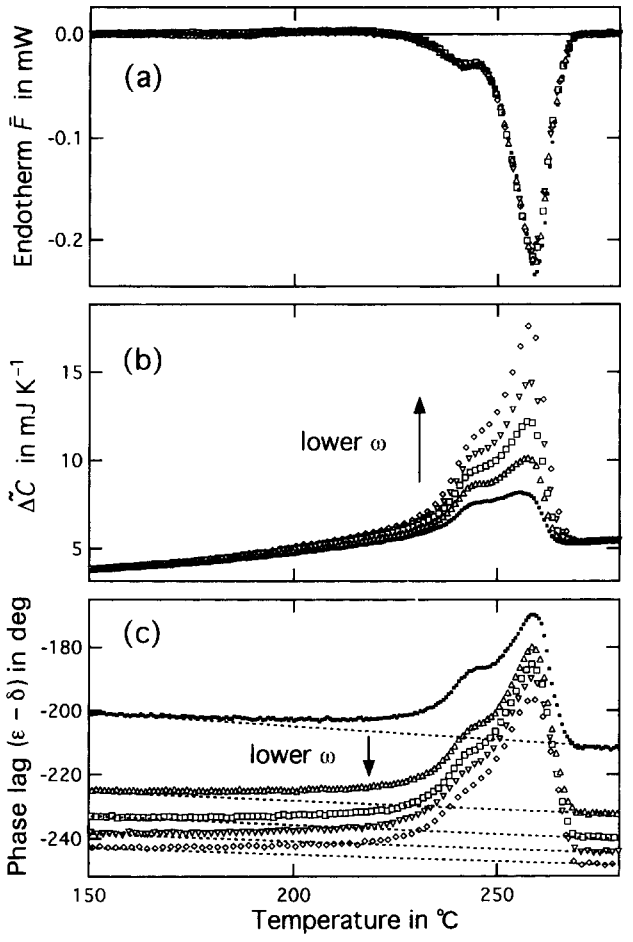

Figure 3 Raw data for t.m.d.s.c. showing the frequency dependence of the melting process of PET crystals of 2.78 mg by heating runs at 1.4 K min^{-1}: (a) endothermic heat flow $\bar{F}$ obtained by a conventional baseline subtraction without the 'reversing' heat flow, (b) the magnitude of the apparent heat capacity $\Delta\tilde{C}$ after the correction for different modulation periods and (c) phase lag ($\epsilon - \delta$). The symbols represent the following modulation periods: 28 (■), 44 (△), 56 (□), 68 (▽) and 84 s (◇). In (c), the dotted lines represent the baselines $(\epsilon - \delta)_0$ determined by the straight lines between the data points at 150 and 280°C

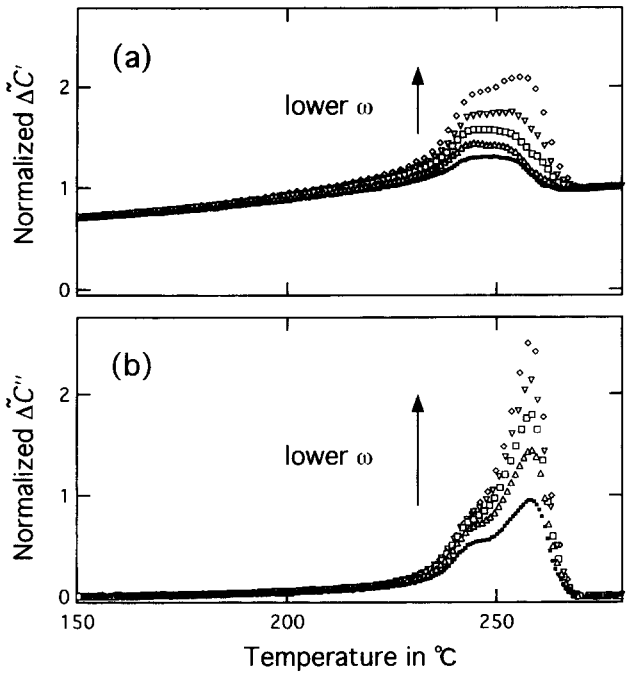

Figure 4 Frequency dependence of (a) the real part $\Delta\tilde{C}'$ and (b) the imaginary part $\Delta\tilde{C}''$ of the apparent heat capacity obtained by the data shown in *Figure 3*. The symbols represent the following modulation periods: 28 (■), 44 (△), 56 (□), 68 (▽) and 84 s (◇). The value of the apparent heat capacity was normalized by that of molten PET at 280°C

the phase lag were large enough, as shown in *Figure 3c*. The baseline of the endothermic heat flow was not corrected for the subtraction of the contribution of heat capacity (the 'reversing' heat flow), because of the reason mentioned in the *Introduction*.

Sample was an amorphous poly(ethylene terephthalate) film supplied by Toyobo. The sample weight was in the range of 2–14 mg, and there was no qualitative difference by weight; the following data are mainly of 2.7–2.9 mg.

Frequency and heating rate dependence of the apparent heat capacity

Figures 3 and 4 show the endothermic heat flow and the apparent heat capacity on heating at the rate of 1.4 K min^{-1} for different periods of modulation. From *Figure 3a*, we can confirm that the endothermic heat flow was not affected by the change of modulation period. On the other hand, both of real and imaginary parts of the apparent heat capacity showed a strong frequency dependence in *Figure 4a,b*, where the real and imaginary parts are defined as,

$$\Delta\tilde{C}e^{-i\alpha} = \Delta\tilde{C}' - i\Delta\tilde{C}'' \qquad (7)$$

This behavior of frequency dependence contrasts with the case of crystallization in which the real part was almost independent of frequency (equation (6)).

Figure 5 shows the frequency dependence of the apparent heat capacity obtained for several different heating rates at the same temperature of 257.0°C; the real and imaginary parts are plotted against modulation period. It is clearly seen from *Figure 5* that the behavior in the frequency dependence has a strong dependence on heating rate.

Non-linearity

Figure 6 shows the ratio of the amplitude of the first and second harmonics of the response in heat flow and that of sample temperature during the melting of PET crystals. It is seen that the ratio of heat flow is comparatively large (ca. several %), while a small ratio of temperature guarantees sinusoidal temperature control. The higher harmonics of heat flow indicate a non-linear response of melting kinetics to temperature modulation, as discussed below.

KINETIC MODELLING OF THE MELTING PROCESS

In the theoretical part, we firstly review our model applied to polymer crystallization which did not show the frequency response of F'_T. Secondly, we summarize the characteristics of the melting of polymer crystals in order to formulate the modelling. The effect of re-crystallization and re-organization is also discussed. Subsequently, we present a kinetic modelling of the melting of polymer crystals and calculate the frequency response of the endothermic heat flow of melting to temperature modulation. The model successfully explains the experimental results as the response in melting kinetics, and provides quite valuable information about re-crystallization and re-organization, utilizing the insensitive nature of the apparent heat capacity to those processes.

A basic model without frequency response in F'_T

If we take the exotherm as a positive heat flow, the heat flow, $\dot{Q}$, to and from the sample can be represented

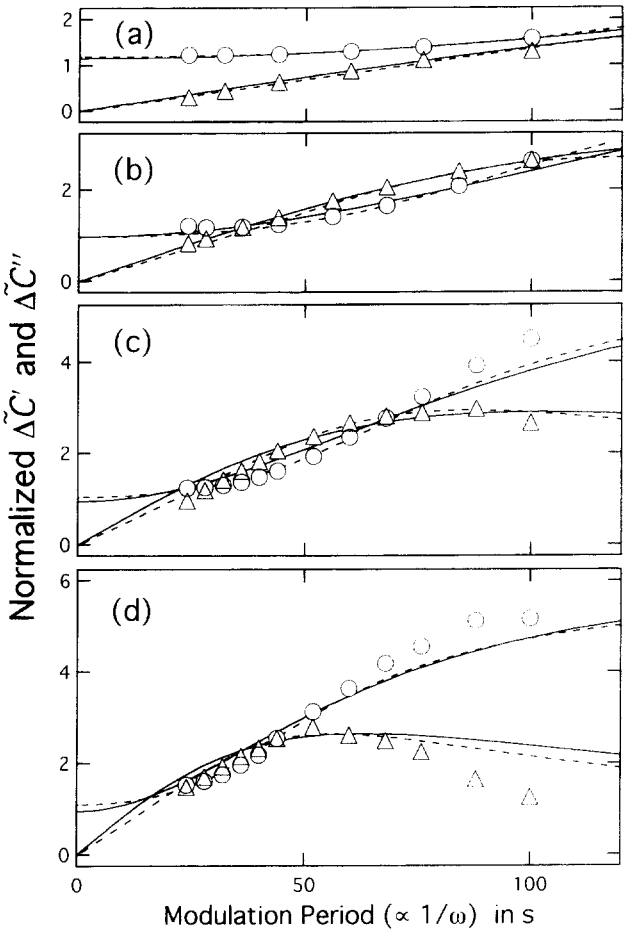

Figure 5 Plots of the real (○) and imaginary (△) parts of the (normalized) apparent heat capacity during the melting process of PET against modulation periods. The data at 257.0°C were taken from the heating runs of the following rates: (a) 0.7, (b) 1.4, (c) 2.0 and (d) 3.0 K min^{-1}. The solid and broken lines are the plots of equations (27) and (33), respectively, with the adjustable parameters of c_p, ϕ_0 and τ_1 or τ_2

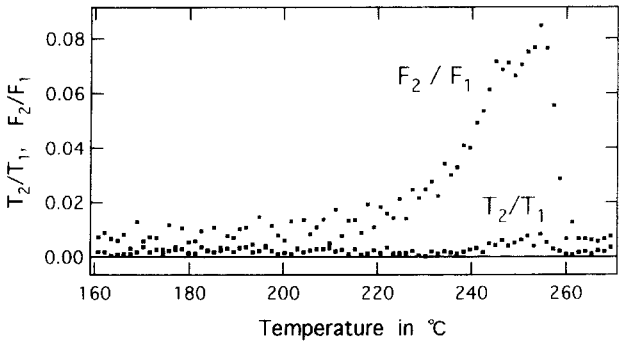

Figure 6 Plots of the ratio of the amplitude of the first and second harmonics of the response in heat flow, F_2/F_1, and that of sample temperature, T_2/T_1, during the melting of PET crystals. The heating rate was 3.0 K min^{-1}. The modulation period was 28 s. The sample weight was 2.36 mg

as follows,

$$\dot{Q} = -mc_p \frac{dT_s}{dt} + F(t) \tag{8}$$

In the equation, $-mc_p dT_s/dt$ is the contribution of heat capacity of sample and the second term $F(t)$ represents exo- or endothermic heat flow. With the heat capacity of mc_p in equation (8), heat flow appears only for a temperature change, dT_s/dt; the response in heat flow changes its sign against increasing and decreasing temperature, and hence the process is reversible. On the other hand, the rate of transformation is not a function of dT_s/dt but of T_s (in other words, the degree of superheating or supercooling), as far as the system is supercooled or superheated. Hence, the exo- or endothermic heat flow due to a transformation is not reversible against small temperature change, but continues the transformation. Instead of the change in the sign of heat flow, temperature change causes a modulation of the rate of transformation. Since the transformation rate is a function of T_s, the exo- or endothermic heat flow will have the following expansion about sample temperature for a small modulation,

$$F(t, T_s) = \bar{F}(t, \bar{T}_s) + F_T'(t, \bar{T}_s)\tilde{T}_s e^{i(\omega t + \epsilon)} \tag{9}$$

where F'_T represents the temperature derivative of the exo- or endothermic heat flow. It should be mentioned that the possibility of the linear expansion was originally pointed out by Reading and coworkers[1–3] and also discussed by Schawe[15]. However, each term of the expansion has not been explained from the view point of the mechanism of phase transition.

By applying a sinusoidal modulation to sample temperature, the modulation components of $\dot{Q}$, $\dot{T}_s$ and F appearing in equation (8) must be in valance, as follows,

$$\tilde{Q}e^{i(\omega t + \delta)} = -mc_p \frac{d}{dt}\tilde{T}_s e^{i(\omega t + \epsilon)} + F_T'\tilde{T}_s e^{i(\omega t + \epsilon)} \tag{10}$$

$$= -\widetilde{\Delta C} e^{-i\alpha} \frac{d}{dt}\tilde{T}_s e^{i(\omega t + \epsilon)}$$

where $\widetilde{\Delta C} e^{-i\alpha}$ defines the apparent heat capacity of the complex quantity expressed in equations (3)–(5). For a sinusoidal modulation,

$$\frac{d}{dt}\tilde{T}_s e^{i(\omega t + \epsilon)}$$

and

$$\tilde{T}_s e^{i(\omega t + \epsilon)}$$

are at right angles each other, and hence F'_T is multiplied by i/ω when translated to the value as an apparent heat capacity in equation (5). The term $(i/\omega)F'_T$ is responsible for the change in the phase lag of the apparent heat capacity during transformations such as crystallization and melting. Concerning the crystallization of polymers (polyethylene and PET), the frequency dependence of the apparent heat capacity was well approximated by equation (6). The dependence confirms the expression of equation (5) with mc_p and F'_T being independent of modulation frequency.

In the apparent heat capacity of $\widetilde{\Delta C} e^{-i\alpha}$ given by equation (5), the true heat capacity, mc_p, can undergo a relaxation process such as glass transition, which gives rise to a negative imaginary part of mc_p as a consequence of irreversibility[16]. The coefficient, F'_T, can also be of complex quantity, depending on the frequency response in the transformation kinetics to temperature modulation.

Melting of polymer crystals

Before proceeding to the modelling of melting kinetics, we shall summarize the characteristics of the melting of polymer crystals[12].

(1) Polymer crystals are quasi-stable having a continuous distribution of non-equilibrium melting points determined mainly by the distributions of lamellar thickness and of molecular weight. The wide

distribution of melting temperatures is responsible for the broad endothermic peak in the melting of polymer crystals, e.g. *Figure 1*. Successive melting of the crystallites is therefore expected for a heating run.

(2) Melting is a fast process completed under low superheating, in contrast with crystallization which usually requires high supercooling (ca. > 10°C). For a limited fraction of crystallites having melting points slightly lower than sample temperature, it is probable to expect the completion of melting in a time interval comparable to the modulation period (20–100 s). Hence, we can expect a frequency response of the kinetics.

(3) In principle, we can think of reversible and irreversible melting of polymer crystals. Irreversible melting is expected for a non-isothermal heating run ($dT_s/dt > 0$); we are concerned with the irreversible process in the present paper. On the other hand, reversible process of melting (and crystallization) is also possible if we apply a modulation around a constant temperature (quasi isothermal mode of constant $\bar{T}_s$) in the melting range[13,14]. In the irreversible melting on a run of heating only ($dT_s/dt > 0$), the response to a temperature modulation only concerns the melting kinetics of superheated crystallites. On the other hand, during the process of reversible melting (and crystallization), we have to consider the response of melting above the melting point and the response of crystallization below the melting point when a temperature modulation is applied around the melting point of a crystallite. It is known that the temperature (superheating or supercooling) dependences of those processes are strongly asymmetric[12] and the reported modulation of heat flow is actually deformed from a sinusoidal shape in its profile[14]. Besides the asymmetry in the melting and crystallization, it is further reported that, on quasi-isothermal measurements, the apparent heat capacity increases due to a (symmetric) response of reversing melting and crystallization on still existing crystals[13,14]. Considering the complexity of the melting phenomena observed by the quasi-isothermal measurements, we expect that the irreversible melting on a run of heating only will be more straightforward.

Re-crystallization and re-organization

We have to consider the contribution of re-crystallization and re-organization because the temperature range of non-equilibrium melting is well below the equilibrium melting temperature.

Firstly, we should make a comment on an additive nature of crystallization and melting in the apparent heat capacity. It is apparent that the exothermic heat flow of re-crystallization and re-organization is subtractive from the endothermic heat flow of melting. On the other hand, the effect in the apparent heat capacity of equation (5) is determined by the sign of the temperature derivative, F'_T, defined in equation (9). If it is ordinary crystallization or melting, the derivative takes a negative value indicating a decrease in exotherm or an increase in endotherm against a rise in temperature. Therefore, the contribution to the apparent capacity of re-crystallization and re-organization makes an additive effect to that of melting.

We may be able to estimate the contribution experimentally, comparing the change in the apparent heat capacity during the melting and ordinary crystallization processes. For PET shown in *Figure 1*, the change in the apparent heat capacity is negligibly small during crystallization compared to the melting peak, mainly because of the smaller magnitude of the temperature derivative, F'_T, of crystallization in equation (5). The temperature dependence of the rate of re-crystallization and re-organization will be similar to that of crystallization, or may be even weaker, because of the existence of still surviving crystals which will serve as the substrate of re-crystallization and re-organization. Therefore, we can reasonably neglect the contribution of re-crystallization and re-organization to the change in the apparent heat capacity in the following calculation concerned with melting.

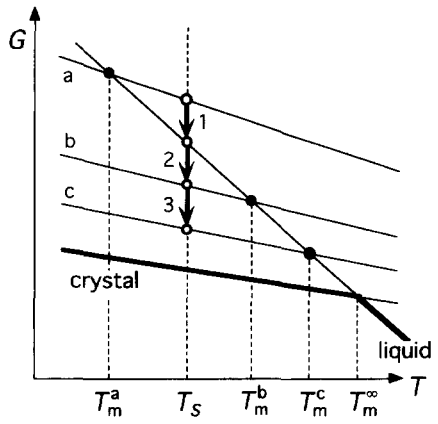

Figure 7 Schematic plots of Gibbs free energy of liquid and crystal in equilibrium (thick lines) and of quasi-stable crystals, **a**, **b** and **c**, (thin lines) against temperature. Process 1 represents the melting of fraction **a** having $T_m < T_s$ and Processes 2 and 3 represent re-crystallization to the fraction **b** and re-organization to the fraction **c**, respectively; both of the fractions **b** and **c** are of $T_m > T_s$

Owing to re-crystallization and re-organization, we also have to consider the change in the distribution of fractions having different melting temperatures. *Figure 7* shows melting, re-crystallization and re-organization on the plots of Gibbs free energy against temperature. Re-crystallization produces a crystal having $T_m > T_s$ from the melt (Process 2) and increases the fractions of $T_m > T_s$. Re-organization (Process 3) will also modify the distribution of the fractions having $T_m > T_s$. It is obvious from *Figure 7* that even though the processes influence the distribution of $T_m > T_s$, the distribution of a superheated fraction having $T_m < T_s$ will not be affected by those processes. Therefore, melting kinetics considered below is not influenced by those processes, though the initial amount of the fraction before melting increases with the processes.

Frequency response in the melting kinetics concerned with F'_T

We define the fraction of the crystallites having the melting temperature in the range from T_m to $T_m + dT_m$, as $\phi(t, T_m)\, dT_m$. The total crystallinity is then expressed by the fractions as,

$$\Phi(t) = \int_0^\infty dT_m \phi(t, T_m) \tag{11}$$

We consider irreversible melting on heating and assume that the melting rate coefficient, R, of a fraction, $\phi(t, T_m)$, is a function of superheating, $\Delta T \equiv T_s - T_m$, expressed as,

$$R = \begin{cases} 0 & \text{for } \Delta T < 0 \\ R(\Delta T) & \Delta T > 0 \end{cases} \tag{12}$$

Utilizing equation (12), the change in the fraction, $\phi(t, T_m)$,

is described by the following differential equation,

$$\frac{d\phi(t,\ T_m)}{dt} = -R\phi(t,\ T_m) \tag{13}$$

For superheating only ($dT_s/dt > 0$), the solution of equation (13) is simply given as,

$$\phi(t,\ T_m) = \phi(0,\ T_m)\exp\left[-\int_0^t R\,dt'\right] \tag{14}$$

As mentioned above, the contribution of re-crystallization and re-organization is not considered in the calculation.

We consider a sinusoidal modulation of temperature expressed in equation (1) with a linear heating, $\bar{T}_s = \beta t$. If we define $\beta t_0 + \tilde{T}_s e^{i\omega t_0} \equiv T_m$, the superheating, ΔT, is given as a function of t_0 and $\Delta t \equiv t - t_0 (> 0)$, as follows,

$$\Delta T(\Delta t,\ t_0) = \beta\Delta t + \tilde{T}_s e^{i\omega t_0}(e^{i\omega\Delta t} - 1) \tag{15}$$

Then, the response in the melting rate coefficient to the small temperature modulation is expanded as,

$$R(\Delta T) = R(\beta\Delta t) + R'(\beta\Delta t)\tilde{T}_s e^{i\omega t_0}(e^{i\omega\Delta t} - 1) \tag{16}$$

$$+ \frac{1}{2}R''(\beta\Delta t)[\tilde{T}_s e^{i\omega t_0}(e^{i\omega\Delta t} - 1)]^2 + \ldots$$

where R' and R'' represent the first and second derivatives of R in terms of ΔT. The crystallinity of each fraction, $\phi(\Delta t > 0,\ t_0)$, given by equation (14) is then approximated, as follows,

$$\phi(\Delta t,\ t_0) = \phi_0 e^{-\int_0^{\Delta t} dx R(\beta x)}\{1 - \tilde{T}_s e^{i\omega t_0}$$

$$\int_0^{\Delta t} dx R'(\beta x)(e^{i\omega x} - 1) + \ldots\} \tag{17}$$

The endothermic heat flow of melting, $F_{melt}(t)$, is given by the time derivative of the degree of the total crystallinity, Φ, multiplied by the enthalpy difference of the system, $\Delta H (> 0)$. In order to calculate the steady response in heat flow, we suppose a hypothetical situation of uniform distribution of the fractions at the initial state, $\phi(0, T_m) = \phi_0$, and the same form of $R(\Delta T)$ for the fractions. For the uniform distribution of the initial fractions, the steady response to a sinusoidal modulation of temperature should be represented by a Fourier series expressed as,

$$F_{melt}(t) = \Delta H\frac{d\Phi}{dt} = \bar{F}_{melt} + F_T'(\omega)\tilde{T}_s e^{i\omega t} + \ldots \tag{18}$$

It can be shown that the assumption is justified for the actual variation in $\phi(0, T_m)$ being negligible in a temperature range larger than $\beta \times$ (Modulation Period) and $2\pi\beta\tau$, where τ represents a characteristic time for the melting of crystallites, as introduced below. The conditions require a quasi-steady state of the melting process within the temperature ranges.

Concerning the requirement of the quasi-steady state of the melting kinetics, the irreversible melting (or irreversible processes in general) needs to be differentiated from the reversible processes of modulation in the case of heat capacity measurement or of the reversible melting and crystallization. For the measurement of heat capacity on heating or cooling, it has been pointed out that the application of MDSC requires the change in the system fast enough to follow the temperature change of the heating or cooling run[17]. It means that the modulation should be around an equilibrium state in the case of heat capacity measurement. For the reversible melting and crystallization, it has also been pointed out that the steady response of the cycles of melting and crystallization must be attained by a modulation around a constant temperature[13,14]. On the other hand, we are concerned with the irreversible melting on heating, namely an irreversible transformation process. The process cannot be in the steady state in the long run, and hence we must consider whether the process can be approximated as a quasi-steady state or not. In the present case of the successive melting of crystallites, the steady state is attained only when the distribution of the melting point is uniform. For the actual distribution of the melting points, the above-mentioned conditions give the criterion for the justification of the quasi-steady state approximation.

From equations (16) and (17), it is obvious that the response in the melting kinetics is essentially non-linear and the Fourier series of $F_{melt}(t)$ in equation (18) should have the higher harmonics. This argument is supported by the experimental evidence of the non-linearity discussed in the section *Experimental Results*. In the following, we are only concerned with the term of the linear response which is related to the apparent heat capacity. The behavior of the higher harmonics will be the subject of further study.

In equation (18), the underlying endothermic heat flow of melting. $\bar{F}_{melt}$, is given by a constant heating rate, $\bar{T}_s = \beta t$. If we define $\beta t_0 \equiv T_m$, the crystallinity of each fraction, $\phi(t,\ T_m)$, becomes a function of $(t - t_0)$. For $t/\tau \gg 1$ under steady state, $\bar{F}_{melt}$ is then represented as follows,

$$\bar{F}_{melt} = \Delta H\int_0^\infty \beta\,dt_0\frac{d\phi(t - t_0)}{dt} = -\Delta H\phi_0\beta \tag{19}$$

On the other hand, the coefficient of the first harmonic, $F'_T(\omega)\tilde{T}_s$, in equation (18) is given by a Fourier integral of $F_{melt}(t)$ as,

$$F_T'(\omega)\tilde{T}_s = \bar{F}_{melt}\frac{\int_{-\infty}^{\infty} dt\, e^{-i\omega t}F_{melt}(t)}{\int_{-\infty}^{\infty} dt\, F_{melt}(t)}$$

$$= \phi_0\beta\int_{-\infty}^{\infty} dt e^{-i\omega t}F_{melt}(t) \tag{20}$$

Using equation (11), the Fourier integral of $F_{melt}(t) = \Delta H(d\Phi/dt)$ is calculated as,

$$\int_{-\infty}^{\infty} dt e^{-i\omega t}F_{melt}(t) = i\omega\Delta H\int_{-\infty}^{\infty} dt e^{-i\omega t}\int_0^\infty dT_m\phi(t,\ T_m)$$

$$= i\omega\Delta H\int_0^\infty dt_0(\beta + i\omega\tilde{T}_s e^{i\omega t_0})e^{-i\omega t_0}$$

$$\int_{-\infty}^{\infty} d(\Delta t)e^{-i\omega\Delta t}\phi(\Delta t,\ t_0) \tag{21}$$

In order to obtain the linear response, $F_T'(\omega)\tilde{T}_s$, to the sinusoidal temperature modulation under steady state, it is only required to select the terms including $\tilde{T}_s$ in the expression of equation (21). Then, taking account of $\phi(\Delta t < 0,\ t_0) = \phi_0$,

$$\int_0^\infty e^{i\omega x}\,dx = \pi\delta(\omega) + \frac{i}{\omega}$$

and

$$\int_0^\infty \phi_0\beta\,dt_0 = 1,$$

the linear response can be calculated. Hereafter, we utilize the following expression of the contribution of the melting kinetics to the apparent heat capacity,

$$\widetilde{\Delta C}e^{-i\alpha} = mc_p + f(\omega) \tag{22}$$

$$f(\omega) \equiv f'(\omega) - if''(\omega) = \frac{i}{\omega}F_T'(\omega) \tag{23}$$

The contribution, $f(\omega)$, is then expressed as follows, for $R' \neq 0$,

$$f(\omega) = \Delta H\phi_0\beta \int_0^\infty dx e^{-i\omega x} e^{-\int_0^x dy R(\beta y)} \int_0^x dy e^{i\omega y} R'(\beta y) \tag{24}$$

and for a constant melting rate coefficient of R_0 ($R'_0 = R''_0 = \ldots = 0$),

$$f_0(\omega) = \frac{\Delta H\phi_0}{1 + i\omega\tau_0} \tag{25}$$

$$\tau_0 \equiv 1/R_0 \tag{26}$$

It is noted that the constant melting rate coefficient means a stepwise change of the rate at $\Delta T = 0$ and corresponds to $R'(\Delta T) = R_0\delta(\Delta T)$ in equation (24).

For the constant melting rate coefficient, $f_0(\omega)$ of equation (25) corresponds to the frequency response function of Debye's type with the characteristic time of $\tau_0 = 1/R$. In this case, the melting process of a fraction is simply expressed as $\phi(\Delta t) = \phi_0 \exp(-R\Delta t)$ from equation (14) and is actually characterized by the time, τ_0. The characteristic time, τ_0, is a constant and does not show the heating rate dependence of the apparent heat capacity shown in *Figure 5*. If the melting rate coefficient shows a superheating dependence, we expect the dependence on heating rate of the characteristic time related to the melting kinetics of a fraction. In the following, we consider two different dependences of melting rate coefficient on superheating, $R_1 = a\Delta T$ and $R_2 = (a/c)(e^{c\Delta T} - 1)$, and calculate the contribution of $f(\omega)$.

The case of $R_1 = a\Delta T$. We assume that the melting rate coefficient follows the simplest dependence on superheating, namely a linear dependence represented as $R_1 = a\Delta T$ for $\Delta T > 0$. Then, the contribution of the melting kinetics, $f_1(\omega)$, is represented as,

$$f_1(\omega) = \frac{\Delta H\phi_0}{\omega\tau_1}\{e^{-(\omega\tau_1)^2} \int_0^{\omega\tau_1} e^{x^2} dx - i\frac{\sqrt{\pi}}{2}(1 - e^{-(\omega\tau_1)^2})\} \tag{27}$$

$$\tau_1 \equiv \left(\frac{1}{2a\beta}\right)^{1/2} \tag{28}$$

In *Figure 8*, the real and imaginary parts of $f_1(\omega)$ are plotted along with the frequency response function of Debye's type, $1/(1 + i\omega\tau)$. Those figures suggest that $f_1(\omega)$ expressed in equation (27) is similar in its behavior to the frequency response function of Debye's type. As we had expected, the superheating dependence of the melting rate coefficient gives rise to the heating rate dependence of the characteristic time: $\tau_1 \propto \beta^{-1/2}$.

We can understand the limiting behaviors of $f_1(\omega)$ shown in *Figure 8*, if we consider the melting of a fraction, $\phi(t, T_m)$ dT, (*Figure 9b,c*) on a heating run shown in *Figure 9a*. In *Figure 9b,c*, we plotted two limiting cases of (i) and (iii) as well as the intermediate one, (ii). Here, the limiting cases are determined by the value of $\tau_1 = 1/(2a\beta)^{1/2}$ which characterizes the melting process of a fraction expressed as $\phi(\Delta t) = \phi_0 \exp(-(\Delta t/2\tau_1)^2)$ from equation (14). For

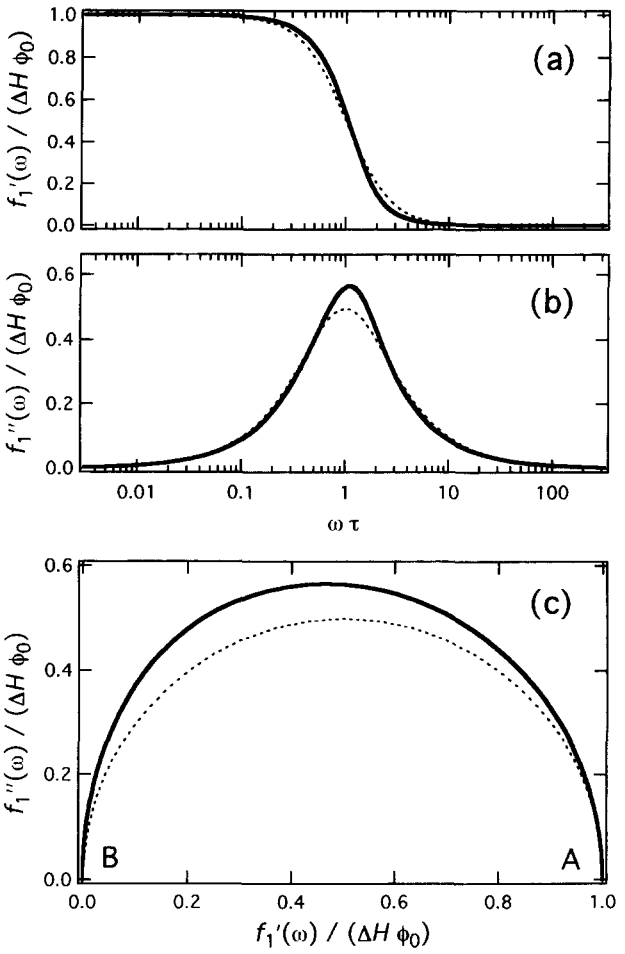

Figure 8 Plots of $f'_1(\omega)$ and $f''_1(\omega)$ of equation (27) (thick lines). The dotted lines represent the plots of frequency response function of Debye's type for the same characteristic time. In (a) and (b), they are plotted against $\log(\omega\tau)$ and the Cole–Cole plot is shown in (c)

$\omega\tau_1 \ll 1$ represented by (i) in *Figure 9b,c*, the fraction completes melting in a time interval much smaller than the modulation period. To sustain the steady response of melting endotherm, we need a continuous distribution of the melting points. In a time interval of dt, fractions of ϕ_0(dT/dt)dt complete melting. Therefore, the response becomes proportional to the change in temperature, dT/dt, and hence the contribution to the apparent heat capacity, $f_1(\omega)$, becomes a real quantity (the phase angle $\alpha \to 0$) for the limiting case of $\omega\tau_1 \ll 1$ (A in *Figure 8c*). For $\omega\tau_1 \gg 1$ represented by (iii) in *Figure 9b,c*, on the other hand, the change in $\phi(t, T_m)$ during the modulation period becomes negligible, and we can expect the change in the melting rate coefficient as the response to temperature modulation. The change follows sample temperature, T_s, and hence $f_1(\omega)$ becomes an imaginary value ($\alpha \to \pi/2$) while the magnitude, $|f_1(\omega)|$, becomes smaller for larger $\omega\tau_1$ (B in *Figure 8c*).

The case of $R_2 = a/c(e^{c\Delta T} - 1)$. Assuming an exponential dependence of $R_2 = (a/c)(e^{c\Delta T} - 1)$, the contribution of the melting kinetics, $f_2(\omega)$, is represented as,

$$f_2(\omega) = \frac{\Delta H\,\phi_0}{1 + \omega\tau_2}\frac{1}{\tau_3}\int_0^\infty dx(e^{x/\tau_2} - e^{-i\omega x})$$

$$\exp\left[-\frac{\tau_2}{\tau_3}(e^{x/\tau_2} - 1 - \frac{x}{\tau_2})\right] \tag{29}$$

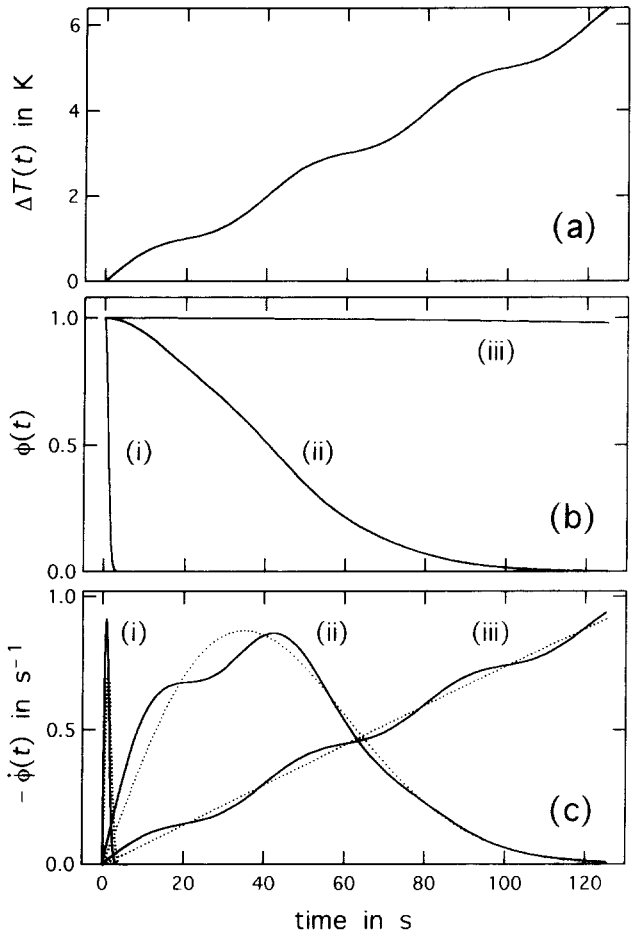

Figure 9 Plots of $\Delta T(t)$, $\phi(t)$ and $-\dot{\phi}(t)$ of equations (13)–(15) for a fraction having $\Delta T = 0$ at $t = 0$. The values of the following parameters are fixed at $\bar{T}_s = \pm 0.2$ K, period = 40 s and $\beta = 3$ K min^{-1}. For (i)–(iii), $a =$ 1000, 1 and 0.003 K^{-1} min^{-1}, which corresponds to $\omega\tau_1 = 0.122$, 3.8 and 70.2, respectively. In (c), the magnitude of $-\dot{\phi}$ for (i), (ii) and (iii) was multiplied by 1.3, 50 and 3×10^3, respectively. The melting rate coefficient, $-\dot{\phi}$, without the modulation is also shown in (c) by dotted lines

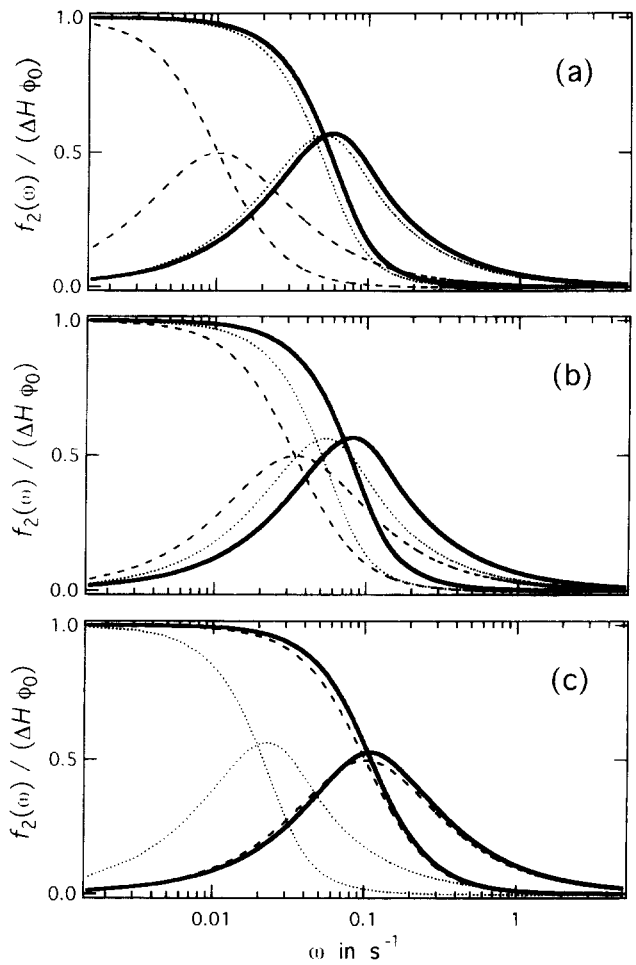

Figure 10 Numerical calculations of the real and imaginary parts of $f_2(\omega)$ of equation (29) (thick lines) for $\tau_2/\tau_3 = 100/10$ (a), 30/30 (b) and 10/500 s/s (c). The dotted and broken lines represent equations (27) and (33), respectively

$$\tau_2 \equiv \frac{1}{\beta c} \tag{30}$$

$$\tau_3 \equiv \frac{c}{a} \tag{31}$$

The numerical calculation of equation (29) shows that the frequency dependence of $f_2(\omega)$ is similar to that of Debye's type (*Figure 10*). Corresponding to the two extreme cases of $\tau_2/\tau_3 \gg 1$ and $\ll 1$, $f_2(\omega)$ is approximated by $f_1(\omega)$ for $\tau_2/\tau_3 \gg 1$,

$$f_2(\omega) \simeq f_1(\omega) \tag{32}$$

with

$$\tau_1 = \left(\frac{\tau_2\tau_3}{2}\right)^{1/2}$$

and by Debye's type for $\tau_2/\tau_3 \ll 1$,

$$f_2(\omega) \simeq \frac{\Delta H\phi_0}{1 + i\omega\tau_2} \tag{33}$$

As mentioned above, the frequency dependence of $f_1(\omega)$ is similar to that of Debye's type. In order to differentiate the two extreme cases, we will need to examine the dependence on heating rate of the characteristic time: $\tau_1 \propto \beta^{-1/2}$ and $\tau_2 \propto \beta^{-1}$.

The different behaviors of $f_2(\omega)$ for the two extreme cases can be understood, if we consider what determines the melting kinetics of a fraction. In the case of $\tau_2 \gg \tau_3$, namely $(a/c) \gg \beta c$, the melting rate coefficient is approximated by the linear dependence of R_1 discussed above, and hence $\tau_1 = 1/(2a\beta)^{1/2}$ characterizes the kinetics. On the other hand, for $\tau_2 \ll \tau_3$, the melting kinetics is determined by the exponential increase in the melting rate coefficient, $R_2(\Delta t) \propto \exp(\beta c\Delta t)$, which is characterized by $\tau_2 = 1/(\beta c)$. Therefore, depending on the ratio of τ_2/τ_3, the characteristic time shows a cross-over change from τ_1 to τ_2 corresponding to the change from linear to exponential dependence on superheating of the melting rate coefficient.

Heat flow of melting and of re-crystallization and re-organization

The present model only concerns the melting process, and hence the underlying endothermic heat flow, $\bar{F}_{\text{melt}}$, represents pure endothermic heat flow of melting. The heat flow, $\bar{F}_{\text{melt}}$, is given by the response in heat flow of melting to linear heating and is related to the apparent heat capacity which is determined by the response to a sinusoidal temperature modulation. Actually, it can be shown from equations (24) and (25) that $f(0) = \Delta H\phi_0$ and the following relationship holds,

$$\bar{F}_{\text{melt}} = -\beta f(0) \tag{34}$$

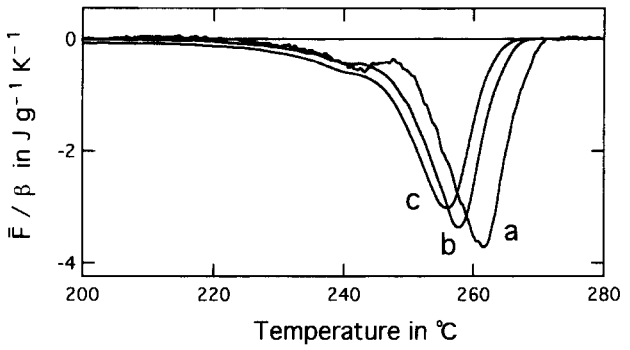

Figure 11 Plots of endothermic heat flow divided by heating rate, $\bar{F}/\beta$, during the melting process of PET crystals for different heating rates of (a) 0.7, (b) 2.0 and (c) 4.5 K min^{-1}. Temperature modulation was not applied

This relationship will be obvious, if we consider the discussion related to *Figure 9*.

Concerning the apparent heat capacity during the process of melting, we have reasonably assumed that the response in the melting kinetics is solely responsible for the change in the apparent heat capacity which is supposed to be insensitive to re-crystallization and re-organization. If it is the case, so-called 'reversing' heat flow of $-\beta\widetilde{\Delta C}$ is expressed as,

$$-\beta\widetilde{\Delta C}(\omega) = -\beta[mc_p + f(\omega)] \tag{35}$$

For $\omega \rightarrow 0$, the 'reversing' heat flow has a limit of,

$$-\beta\widetilde{\Delta C}(0) = -\beta mc_p + \bar{F}_{\text{melt}} \tag{36}$$

which comprises the contribution of specific heat and the pure endothermic heat flow of melting. Actually, in *Figure 2*, the 'reversing' heat flow seems to have a limit for longer modulation periods.

On the other hand, the total heat flow, $\bar{Q}$, of t.m.d.s.c. is equivalent to the heat flow of a conventional d.s.c. and comprises the contribution of specific heat, the endothermic heat flow of melting and the exothermic heat flow of re-crystallization and re-organization, $F_{\text{exo}}(>0)$, as expressed in the following,

$$\bar{Q} = -\beta mc_p + \bar{F}_{\text{melt}} + F_{\text{exo}} \tag{37}$$

$$= -\beta\widetilde{\Delta C}(0) + F_{\text{exo}}$$

From the relationship, it can be said that the absolute value of the total heat flow must be smaller than that of the 'reversing' heat flow extrapolated to $\omega \rightarrow 0$; namely

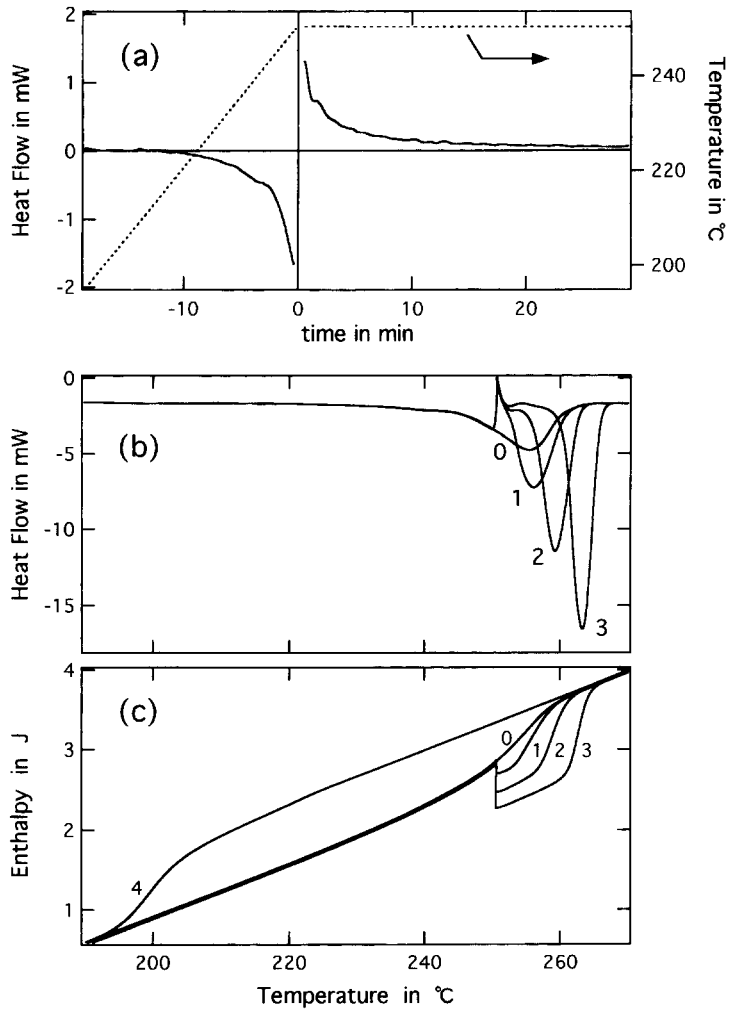

Figure 12 Plots of (a) heat flow (solid line) and sample temperature (dotted line) against run time for a standard d.s.c. without modulation. The sample temperature was raised to 250.0°C at 3.0 K min^{-1} and then kept at that temperature isothermally. In (b) and (c), heat flow and its integration (enthalpy) are shown for heating runs at 3.0 K min^{-1} interrupted by the isothermal annealing at 250.0°C for (0) 0, (1), 5, (2) 50 and (3) 500 min. In (c), the line (4) represents the change in enthalpy for a cooling run at 3.0 K min^{-1} preceding the heating runs. The sample weight was 17.17 mg

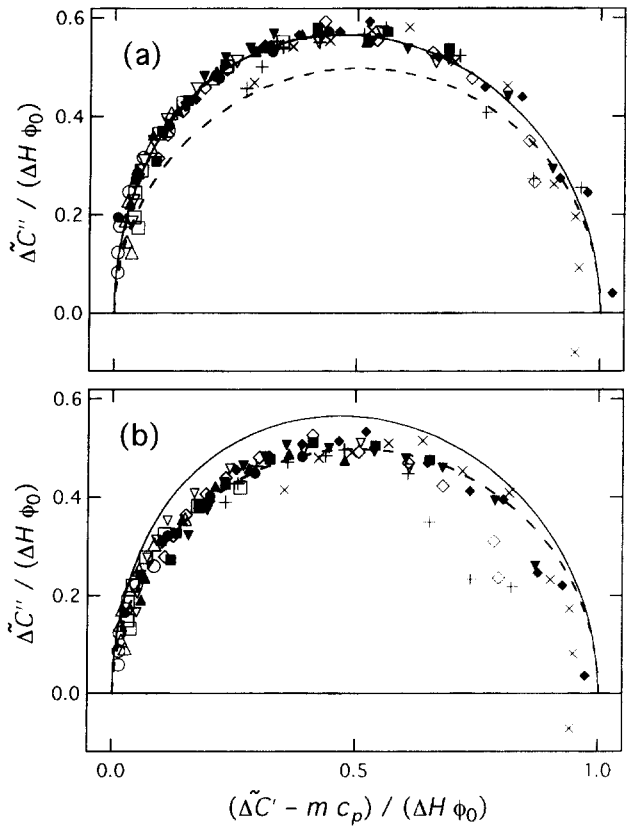

Figure 13 Cole–Cole plot of the real and imaginary parts of the apparent heat capacity such as shown in *Figure 5* taken at 240.0 and 257.0°C for different heating rates. The symbols represent the following heating rates: 0.7 (●,○), 1.0 (▲,△), 1.4 (■,□), 2.0 (▼,▽), 3.0 (◆,◇) and 4.5 K min^{-1} (×, +). The filled and open symbols correspond to the data at 240.0 and 257.0°C, respectively. With the adjustable parameters of c_p, ϕ_0 and τ_1 or τ_2, the data points were fitted to the solid line representing equation (27) in (a) and to the broken line of equation (33) in (b)

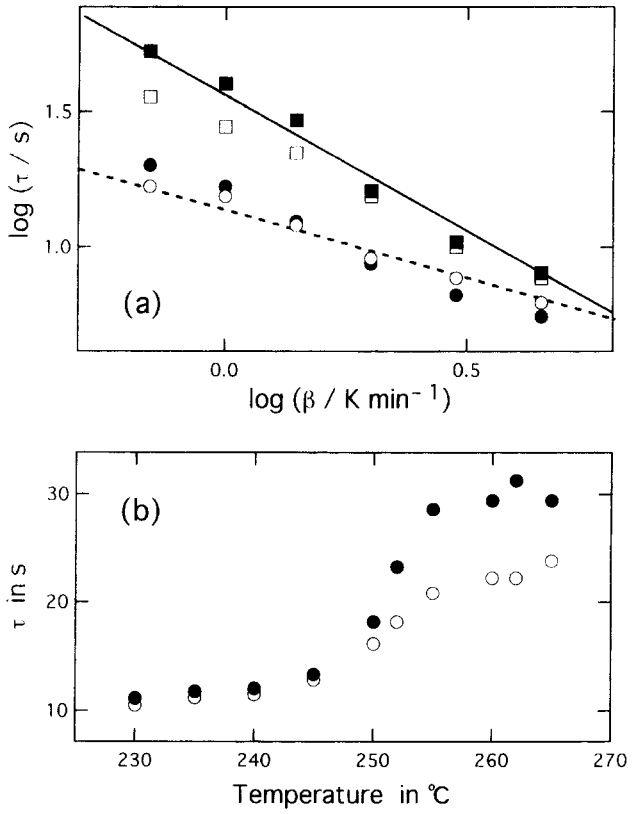

Figure 14 Logarithmic plots of the characteristic time τ chosen for the fitting such as shown in *Figure 5* against (a) heating rate β and (b) temperature. In (a), the symbols represent the values determined for the temperatures of 240°C (○,●) and 257°C (□,■), and in (b) the values were for the heating rate of 1.4 (○,●) K min^{-1}. The open and filled symbols correspond to the fitting to equations (27) and (33) of the apparent heat capacity, respectively. The slopes of the solid and broken lines in (a) are −1.0 and − 0.5, respectively

$|\bar{Q}| \leq |\beta\Delta\tilde{C}(0)|$. This will be the reason for the anomalous relationship between the 'reversing' heat flow and the total heat flow shown in *Figure 2*.

As a consequence of the argument, it is further expected that the corresponding 'non-reversing' heat flow, $\dot{Q} - [-\beta\Delta C(0)]$, is given by the pure exothermic heat flow of re-crystallization and re-organization, F_{exo}. Therefore, by examining the behavior of the 'reversing' and 'non-reversing' heat flows, t.m.d.s.c. enables us to elucidate the endothermic heat flow of melting and the exothermic heat flow of re-crystallization and re-organization, while the total heat flow only gives the sum. It should be mentioned that, since both of the 'reversing' and the 'non-reversing' heat flows are due to the response in irreversible transformations such as melting, re-crystallization and re-organization, the terminology will be misleading for the transformation processes.

Application of the model to the melting of PET crystals

For the melting of PET crystals, we expect a considerable amount of exothermic heat flow of re-crystallization and re-organization[12]. Actually, *Figure 11* shows that the melting peak shifts to higher temperature for slower heating rate because of re-crystallization and/or re-organization. *Figure 12* also shows the direct evidence of re-crystallization and/or re-organization in the temperature range of the melting peak. For those reasons, the endotherm does not correspond to the pure endothermic heat flow of melting, $\bar{F}_{melt} = -\beta\Delta H\phi_0$, and hence ϕ_0 becomes an adjustable parameter of the fitting to the frequency response functions of equations (25), (27) and (33).

In *Figure 5*, the frequency dependence of the real and imaginary parts of the apparent heat capacity has been fitted to equations (22) and (27) or equation (33) with the adjustable parameters of c_p, ϕ_0 and τ_1 or τ_2. *Figure 13a,b* shows the fitting to equations (27) and (33), respectively, in Cole–Cole plots for several different heating rates at 240.0 and 257.0°C. These figures indicate that the frequency dependence can be fitted to both equations (27) and (33) by choosing appropriate values for the parameters. In order to distinguish the difference, we need to examine the dependence on heating rate of the characteristic time; the change in the characteristic time for different heating rates is clearly seen from the shift of the data points for the same range of modulation periods of 28–100 s.

The characteristic time determined by the fitting of the data is plotted in *Figure 14a* against heating rate at three different temperatures. At higher temperatures around the melting peak, the dependence can be fitted to $\tau \propto \beta^{-1}$ (exponential dependence on superheating of the melting rate coefficient), while at lower temperatures to $\tau \propto \beta^{-1/2}$ (linear dependence). Since the exponential dependence on superheating should also be approximated by a linear dependence for superheating low enough, the exponential dependence at higher temperatures means that higher superheating is required for the complete melting at higher temperatures. Actually, in the plot against temperature shown in *Figure 14b*, it is seen that the characteristic time becomes

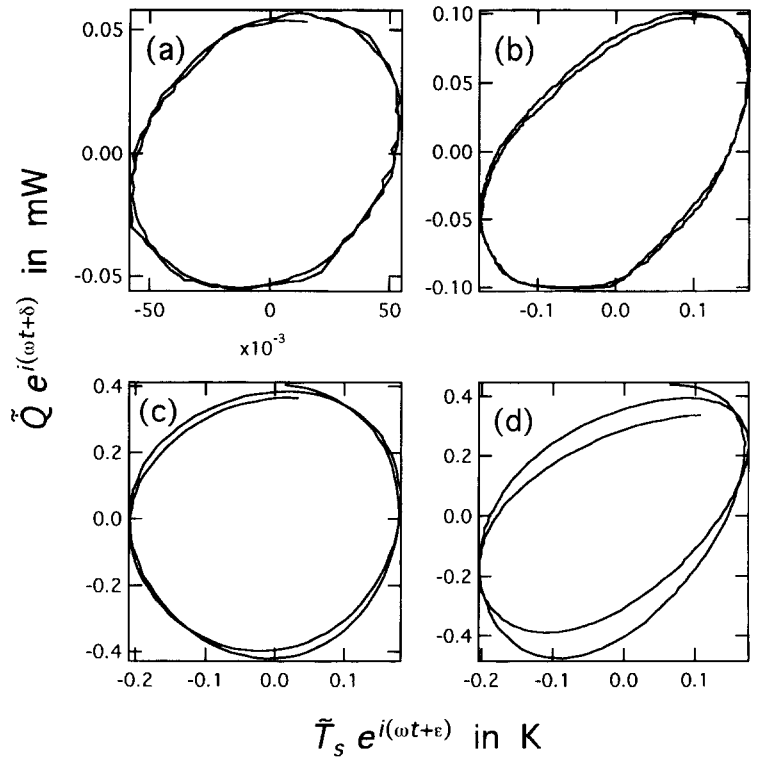

Figure 15 Lissajous diagrams of the modulation component of heat flow during the melting peak plotted against that of sample temperature. The two cycles of the modulation are plotted. The heating rate and the modulation period of t.m.d.s.c. are the following: (a) 0.7 K min^{-1} and 32 s, (b) 0.7 K min^{-1} and 100 s, (c) 4.5 K min^{-1} and 32 s and (d) 4.5 K min^{-1} and 52 s

longer for higher temperatures. We expect the melting of original crystals at lower temperatures and that of re-crystallized or re-organized ones at higher temperatures, and hence the present result indicates slower melting of the re-crystallized or re-organized crystals at low superheating.

Here, we consider the conditions of quasi-steady state required for the application of the present model. For the present experiments, the temperature ranges of $\beta \times$ (Modulation Period) and $2\pi\beta\tau$ are from 0.28 K (Period = 24 s, β = 0.7 K s^{-1}) to 7.5 K (Period = 100 s, β = 4.5 K s^{-1}) and from 1.2 K (τ = 17 s at 240°C, β = 0.7 K s^{-1}) to 4.5 K (τ = 43 s at 262°C, β = 1.0 K s^{-1}), respectively. The change in the apparent heat capacity shown in *Figure 4* is expected to be negligible in the temperature range. The first condition can be judged by plotting a Lissajous diagram of the modulated heat flow against the modulated sample temperature, as shown in *Figure 15* where the two cycles of the data during the melting peak are plotted. Considering the divergence from a closed loop in *Figure 15d*, the maximum range of 7.5 K required for the fastest heating rate seems to exceed the limit, and it may be the reason for the deviation of the data points in *Figure 5* from the fitting curves for faster heating rates and longer modulation periods. The limit of the applicability may also explain the negative $\widetilde{\Delta C}''$ for the fastest heating rate shown in *Figure 13*. Because of the limit of the applicability, we have to use shorter modulation periods and resort to the extrapolation to $\omega \rightarrow 0$ when we discuss the limiting behavior of the 'reversing' and 'non-reversing' heat flow.

Figure 16 shows the plots of the 'reversing' heat flow extrapolated to $\omega \rightarrow 0$, namely $-\beta(mc_p + \Delta H\phi_0)$, and the corresponding 'non-reversing' heat flow, using the values of c_p and ϕ_0 determined by the fittings at each temperature. It is noted that, if the variation in $\phi(0, T_m)$ is small enough, the

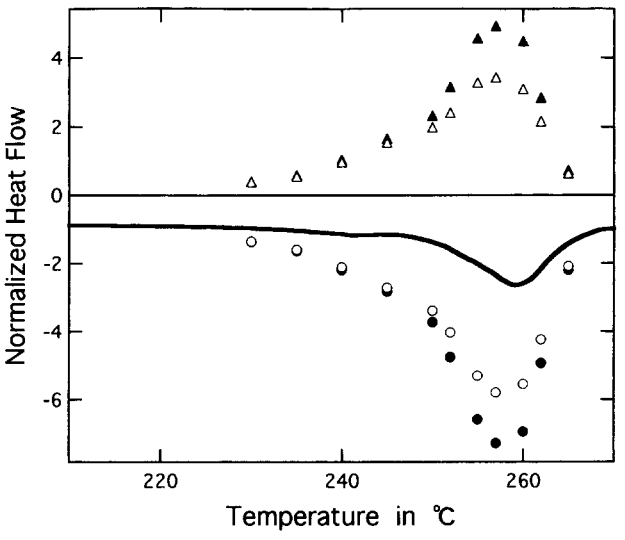

Figure 16 Plots of the total heat flow $\bar{Q}$ (thick line), the 'reversing' heat flow extrapolated to $\omega \rightarrow 0$, $-\beta[mc_p + \Delta H\phi_0]$, (○,●) and the corresponding 'non-reversing' heat flow (△,▲) for the heating rate of 1.4 K min^{-1}. The values of c_p and ϕ_0 for the open and filled symbols were determined by the fitting to equations (27) and (33) of the apparent heat capacity, respectively. The heat flow was normalized by the total heat flow of molten PET at 280°C. The sample weight was 2.78 mg

change in $\phi(0, T_m)$ with temperature is not contradictory to the assumption of a uniform distribution of the melting point of fractions. In *Figure 16*, pure endothermic heat flow of melting appears as the extrapolated 'reversing' heat flow, and pure exothermic heat flow of re-crystallization and re-organization as the corresponding 'non-reversing' heat flow. As mentioned in the section *Heat flow of melting and of re-crystallization and re-organization*, the extrapolated 'reversing' heat flow is actually similar in its

shape and magnitude to the limiting profile of the 'reversing' heat flow for longer modulation periods shown in *Figure 2*. Re-crystallization and re-organization at lower temperatures is clearly seen in this plot, while in the total heat flow the endothermic heat flow of melting cancels out the exothermic heat flow of re-crystallization and re-organization in the temperature range.

DISCUSSION AND CONCLUSION

We have examined the irreversible melting of polymer crystals, utilizing the apparent heat capacity of complex quantity obtained by t.m.d.s.c. The melting of PET crystals showed a strong dependence on frequency and heating rate of the apparent heat capacity. We have argued that the frequency dependence should be explained as a frequency response in the melting kinetics concerned with F'_T.

In order to clarify the physical meaning of the frequency response in the apparent heat capacity, we have presented a detailed modelling of the melting kinetics of polymer crystals having a continuous distribution of the melting points. The frequency response in the melting kinetics to sinusoidal temperature modulation has been examined for a constant melting rate coefficient, a linear dependence on superheating of the melting rate coefficient and an exponential dependence. The modelling produces the frequency dependence similar in its behavior to that of Debye's type and introduces a characteristic time dependent on heating rate, β. The dependence on heating rate of the characteristic time is expressed as $\tau \propto \beta^x$ where $-1 \leq x \leq 0$. Experimentally, the exponent of the heating rate dependence was within a range from $-1/2$ to -1, and depends on temperature.

Concerning the effect of re-crystallization and re-organization during the melting process, it is reasonably assumed that the apparent heat capacity is insensitive to those processes compared to melting. Utilizing the difference in sensitivity, we are able to separate the endothermic heat flow of melting from the exothermic heat flow of re-crystallization and re-organization. Using the conventional terminology of t.m.d.s.c., it means that the peak in the 'reversing' heat flow extrapolated to $\omega \rightarrow 0$ gives the pure endothermic heat flow of melting and the corresponding 'non-reversing' heat flow represents the exothermic heat flow of re-crystallization and re-organization.

Compared to the process of crystallization, it has been quite difficult to examine the melting behavior of polymer crystals because of the non-equilibrium nature of melting, such as the wide distribution of melting temperature and the occurrence of re-crystallization and re-organization. Therefore, the details of the melting kinetics, e.g. superheating dependence of the melting rate coefficient, have not been the subject of d.s.c., microscopy or other conventional methods. An exceptional case was the melting of extended chain crystals of polyethylene having a well defined melting point[18]; the examined melting rate coefficient showed a non-linear dependence on superheating. T.m.d.s.c. enables us to study the melting kinetics under more common conditions and will be a quite useful tool for the investigation of melting process.

ACKNOWLEDGEMENTS

The authors thank Mr K. Sasaki (Toyobo Co. Ltd.) for the kind supply of the amorphous poly(ethylene terephthalate) films. This work was partly supported by a Grant-in-Aid for Scientific Research from the Ministry of Education, Science and Culture of Japan and by NEDO International Joint Research Program.

REFERENCES

1. Gill, P. S., Sauerbrunn, S. R. and Reading, M., *J. Therm. Anal.*, 1993, **40**, 931.
2. Reading, M., Elliott, D. and Hill, V. L., *J. Therm. Anal.*, 1993, **40**, 949.
3. Reading, M., Luget, A. and Wilson, R., *Thermochim. Acta*, 1994, **238**, 295.
4. Wunderlich, B., Jin, Y. and Boller, A., *Thermochim. Acta*, 1994, **238**, 277.
5. Boller, A., Jin, Y. and Wunderlich, B., *J. Therm. Anal.*, 1994, **42**, 307.
6. Hatta, I., *Jpn. J. Appl. Phys.*, 1994, **33**, L686.
7. Toda, A., Oda, T., Hikosaka, M. and Saruyama, Y., *Thermochim. Acta*, 1997, **293**, 47.
8. Toda, A., Tomita, C., Hikosaka, M. and Saruyama, Y., *Polymer*, 1997, **38**, 2849.
9. Toda, A., Tomita, C., Hikosaka, M. and Saruyama, Y., *Polymer*, 1998, **39**, 1439.
10. Toda, A., Oda, T., Hikosaka, M. and Saruyama, Y., *Polymer*, 1997, **38**, 231.
11. Saruyama, Y., *J. Therm. Anal.*, 1997, **49**, 139.
12. Wunderlich, B., *Macromolecular Physics*, Vol. 3. Academic Press, New York, 1976.
13. Okazaki, I. and Wunderlich, B., *Macromolecules*, 1997, **30**, 1758.
14. Ishikiriyama, K. and Wunderlich, B., *Macromolecules*, 1997, **30**, 4126.
15. Schawe, J. E. K., *Thermochim. Acta*, 1995, **260**, 1.
16. Birge, N. O. and Nagel, S. R., *Phys. Rev. Lett.*, 1985, **54**, 2674.
17. Wunderlich, B., Boller, A., Okazaki, I. and Kreitmeier, S., *Thermochim. Acta*, 1996, **282/283**, 143.
18. Hellmuth, E. and Wunderlich, B., *J. Appl. Phys.*, 1965, **36**, 3039.